M/Q = 17 amu e^{-1}. The scan at 1045 U.T. showed very few ions at the higher masses because the plasma flow speed was below the low-velocity threshold of the instrument (80 km sec^{-1}) between 1050 and 1110 U.T. when in the comet tail.

All four scans show peaks in the mass range occupied by ions of the water group (OH^+, H_2O^+, H_3O^+), which were much more abundant than O^+. H_2O^+ appeared to be the most abundant ion in the mass range of the instrument, and we attribute the shoulder on the high mass side of the H_2O^+ peak at H_3O^+. The scan at 1106 U.T. showed a small but significant peak near M/Q = 28 amu e^{-1}, probably due to CO^+ or HCO^+. Both H_2O^+ and CO^+ have been observed spectroscopically in comets (*3*), and H_3O^+ is a prominent constituent in models (*15–17*).

The scans at 1023 and 1106 U.T. show a significant peak at 23.5 to 25 amu e^{-1}. While this could be due to a sudden density fluctuation of at least a factor of 5, this seems unlikely since the spacecraft was well clear of the comet tail at the times of the observations (1038 and 1119 U.T., respectively). The significance of this M/Q peak can be judged from the contour plot in Fig. 5. There is a well-developed and isolated peak at 23.5 amu $e^{-1} \leq M/Q \leq$ 25 amu e^{-1} to which more than six different bins in the M/Q versus V plane contribute. The size of this peak relative to that attributed to H_2O^+ makes interpretation difficult, but a possible candidate in this mass range is Na^+. Atomic sodium (23 amu e^{-1}) has been observed in cometary spectra, but, with rare exceptions (*18*), only in comets close to the sun. Although the abundance of sodium is small, the rate of ionization is large, and, once formed, Na^+ has a long lifetime. Thus the relative abundance of Na^+ may be strongly enhanced in comparison to the molecular ions. Another candidate for this peak could be C_2^+ (24 amu e^{-1}); its neutral counterpart is regularly observed in comets, although Giacobini-Zinner has anomalously low abundances of C_2; furthermore, the rate of photodissociation is several times that of photoionization for C_2.

The velocities and velocity widths of the ions in each of the mass peaks are also evident in Fig. 5. The variation of the velocities of the different ions may simply be due to the fact that the ions were sampled at different distances from the tail axis or from their source and thus could reflect differences in ion production rates and subsequent interactions with the ambient flow field. The ion velocity widths are small compared to the mean velocities. To decide whether this is characteristic of the local conditions or is a cumulative effect, information about the direction from which the ions are flowing is needed. The peaks visible in the scans at 1023, 1106, and 1127 U.T. in Fig. 4 show some variations in M/Q position. While some of these variations may be due to changes in the angle between the plasma flow axis and the instrument axis, we do not rule out the possibility that the composition may vary with the distance from the comet axis.

The results obtained by the ICI at the encounter with Giacobini-Zinner show that the comet fits the generally suggested picture of cometary structure and interaction quite well, with the exception of the unexpectedly large peak tentatively attributed to Na^+.

REFERENCES AND NOTES

1. M. A'Hearn, in *Comets*, L. L. Wilkening, Ed. (Univ. of Arizona Press, Tucson, AZ, 1982), p. 433.
2. D. A. Mendis, H. L. F. Houpis, M. L. Marconi, *Fundam. Cosmic Phys.* **10**, 1 (1985).
3. S. Wyckoff, in *Comets*, L. L. Wilkening, Ed. (Univ. of Arizona Press, Tucson, AZ, 1982), p. 25.
4. L. H. Brace *et al.*, in *Venus*, D. M. Hunten *et al.*, Eds. (Univ. of Arizona Press, Tucson, AZ, 1983), p. 778; C. T. Russell and O. Vaisberg, *ibid.*, p. 873.
5. R. E. Hartle *et al.*, *J. Geophys. Res.* **87**, 1383 (1982).
6. A. A. Galeev, T. E. Cravens, T. I. Gombosi, *Astrophys. J.* **289**, 807 (1985).
7. M. A. Coplan, K. W. Ogilvie, P. A. Bochsler, and J. Geiss [*IEEE Trans. Geosci. Electron.* **9** (No. 16), 185 (1978)] described the construction and calibration of the ICI.
8. S. Kunz, P. Bochsler, J. Geiss, K. W. Ogilvie, and M. A. Coplan [*Sol. Phys.* **88**, 359 (1983)] described the use of the ICI for measurements in the solar wind.
9. K. W. Ogilvie, M. A. Coplan, R. D. Zwickl, *J. Geophys. Res.* **87**, 7363 (1982).
10. K. W. Ogilvie and M. A. Coplan, *Geophys. Res. Lett.* **11**, 347 (1984).
11. N. Meyer-Vernet *et al.*, *Science* **232**, 370 (1986).
12. S. Bame *et al.*, *ibid.*, p. 356.
13. F. L. Scarf *et al.*, *ibid.*, p. 377.
14. J. A. Fedder *et al.*, *Eos* **67**, 17 (1986).
15. W. F. Heubner and P. T. Giguere, *Astrophys. J.* **258**, 753 (1980).
16. W.-H. Ip, *Proc. Int. Meet. Giotto Mission* (ESA SP-169, 1981), p. 79.
17. M. L. Marconi and D. A. Mendis, *Astrophys. J.* **282**, 445 (1984).
18. M. Oppenheimer, *ibid.* **240**, 923 (1980).

19. We thank the many persons, especially those associated with the ICE project, who made this highly successful encounter possible, and T. E. Cravens, W.-H. Ip, and M. F. A'Hearn for helpful comments on the manuscript. P.B. and J.G. thank the Swiss National Science Foundation for support.

20 November 1985; accepted 5 February 1986

Plasma Wave Observations at Comet Giacobini-Zinner

FREDERICK L. SCARF, FERDINAND V. CORONITI, CHARLES F. KENNEL, DONALD A. GURNETT, WING-HUEN IP, EDWARD J. SMITH

The plasma wave instrument on the International Cometary Explorer (ICE) detected bursts of strong ion acoustic waves almost continuously when the spacecraft was within 2 million kilometers of the nucleus of comet Giacobini-Zinner. Electromagnetic whistlers and low-level electron plasma oscillations were also observed in this vast region that appears to be associated with heavy ion pickup. As ICE came closer to the anticipated location of the bow shock, the electromagnetic and electrostatic wave levels increased significantly, but even in the midst of this turbulence the wave instrument detected structures with familiar bow shock characteristics that were well correlated with observations of localized electron heating phenomena. Just beyond the visible coma, broadband waves with amplitudes as high as any ever detected by the ICE plasma wave instrument were recorded. These waves may account for the significant electron heating observed in this region by the ICE plasma probe, and these observations of strong wave-particle interactions may provide answers to long-standing questions concerning ionization processes in the vicinity of the coma. Near closest approach, the plasma wave instrument detected broadband electrostatic noise and a changing pattern of weak electron plasma oscillations that yielded a density profile for the outer layers of the cold plasma tail. Near the tail axis the plasma wave instrument also detected a nonuniform flux of dust impacts, and a preliminary profile of the Giacobini-Zinner dust distribution for micrometer-sized particles is presented.

IT WAS ALWAYS ANTICIPATED THAT THE encounter of the International Cometary Explorer (ICE) with comet Giacobini-Zinner would yield important new information about the plasma physics of the solar wind–comet interaction (*1*), but the actual flyby revealed a surprising strength for the interaction and an unexpected size for the coupling region. The ICE plasma wave instrument detected turbulence associated with fluxes of energetic ions in a pickup region that extended more than 4×10^6 km from the comet nucleus. As ICE approached to within several hundred thousand kilometers of the nucleus, these turbulence levels

F. L. Scarf, F. V. Coroniti, C. F. Kennel, TRW Space and Technology Group, Redondo Beach, CA 90278.
D. A. Gurnett, University of Iowa, Iowa City, IA 52242.
W.-H. Ip, Max-Planck-Institut für Aeronomie, Lindau, West Germany.
E. J. Smith, Jet Propulsion Laboratory, Pasadena, CA 91109.

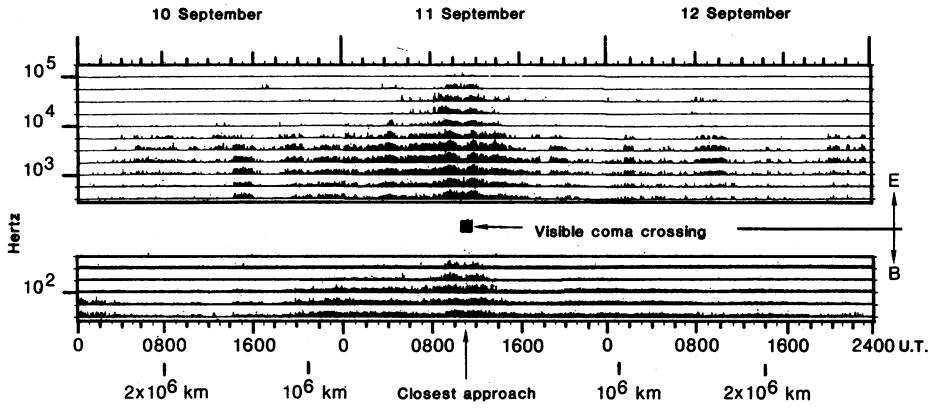

Fig. 1. Overview of plasma wave observations (128-second peak amplitudes in 11 electric field channels and five magnetic field channels) for a 3-day period centered around closest approach to comet Giacobini-Zinner at 1102 U.T., 11 September 1985. The detection of enhanced electrostatic and electromagnetic wave levels throughout the 3-day interval is interpreted in terms of the traversal of a vast pickup region where cometary ions interact strongly with the solar wind.

became so strong and continuous that it was difficult to identify thin bow shock structures. Closer to the nucleus, even higher plasma wave amplitudes were detected as ICE traversed a region of very strong comet–solar wind coupling; electrostatic and electromagnetic wave levels measured just beyond the visible coma were as intense as any signals previously recorded by this wave instrument.

In addition, the two wave instruments on ICE provided profiles of the cold plasma tail, as did similar instruments in the cases of the Io torus at Jupiter (*2*) and the Titan exosphere (*3*). Finally, the ICE plasma wave instrument successfully detected dust impacts at Giacobini-Zinner, just as the Voyager 2 wave instrument had detected dust at Saturn's rings (*4*).

The ICE measurements at Giacobini-Zinner indicate that many important cometary processes are influenced by microscopic plasma physics phenomena to an extent not anticipated in fluid dynamic or magnetohydrodynamic models.

Overall interaction region. For the encounter with Giacobini-Zinner, the ICE plasma wave instrument was operated in its customary cruise mode with the 16-channel spectrum analyzer (18 Hz to 100 kHz) connected to one of the 90-m (tip-to-tip) electric antenna systems and the eight-channel analyzer (18 Hz to 1 kHz) connected to the magnetic search coil (*5*). The search coil output also went to a spectrum analyzer in the vector helium magnetometer experiment; this unit has channels at 0.32 Hz (the spacecraft spin rate), 3.2 Hz, and 8.8 Hz. At the spacecraft telemetry rate of 1 kbit sec^{-1}, we obtained one 16-channel E-field spectrum every second, one eight-channel B-field spectrum every 32 seconds, and one three-channel B-field spectrum every 64 seconds.

Long before closest approach, ICE started to detect wave activity related to the comet, and similar signals were observed after the encounter (Fig. 1). Mid-frequency electric field turbulence started near 0400 universal time (U.T.) on 10 September, when ICE was 2.3×10^6 km from the nucleus, and the E-field levels increased nearly continuously until ICE was within 1 hour of closest approach. Some of the obvious changes in the wave activity during this period were related to varying interplanetary conditions, such as those at 1400 U.T. on 10 September, which were associated with a solar wind discontinuity. However, since the magnetic field was generally not oriented in the spacecraft-comet direction during this 3-day interval, these waves do not represent the customary foreshock turbulence, which is generated by reflected or accelerated solar wind ions; instead, we associate most of this turbulence with passage through a pickup region containing energetic cometary ions.

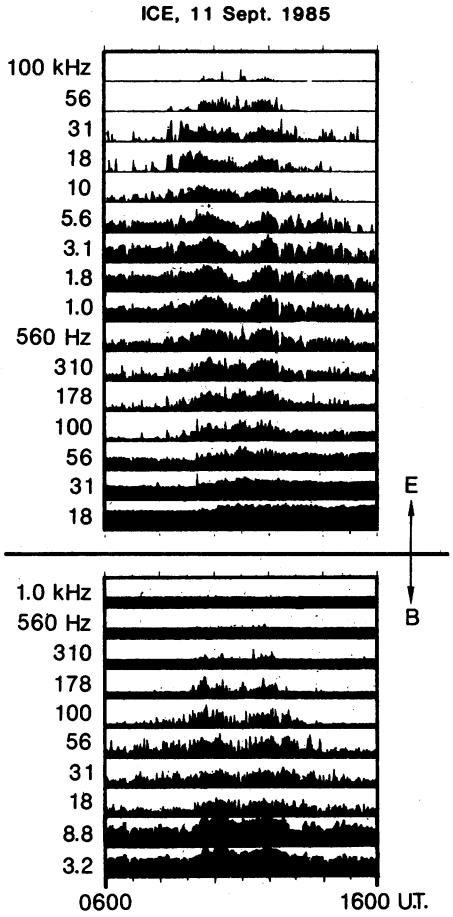

The plasma wave activity after encounter was generally similar to that detected earlier. During the ICE outbound pass, the E-field turbulence levels were considerably more variable and the magnetic sensor provided the most continuous information on the extent of the region affected by cometary ions. (On 10 September the magnetic turbulence level was also elevated at large distances, but there was no clear change at 0400 U.T., when the electrostatic wave activity started to become more or less continuous.) On 12 September, the low-frequency magnetic activity remained high until 2300 U.T., when ICE was at a distance of 2.7×10^6 km, which we interpret as the end of the primary comet-related disturbance that persisted continuously from the time of closest approach. In fact, very similar magnetic activity was detected from 0500 to 1800 U.T. on 13 September, suggesting that strong interactions occurred to a distance of at least 4.3×10^6 km from the nucleus.

The energetic particle detectors were generally able to determine that this extended region of disturbance contained heavy ions having energies greater than 30 keV (*6*). Ip (*7*) showed that significant concentrations of O^+ and OH^+ would persist to a distance of 2×10^6 km for a comet with a gas output of about 5×10^{28} molecules per second; if these heavy ions were picked up by the solar wind, then they would have typical energies of 20 to 30 keV and the resulting nonthermal plasma distributions could readily produce the observed ion acoustic waves as well as the low-frequency magnetic turbulence. Thus we conclude that, during a 4-day period, ICE detected electric and magnetic

Fig. 2. Details of the E- and B-wave measurements within 375,000 km of closest approach. Each panel has a plot of the peak amplitude measured in a 128-second interval. For all 16 E-field channels and the top eight B-field channels the vertical scale corresponds to a variation of nine orders of magnitude in wave energy; the two lowest frequency B-field channels (which show saturation here) have somewhat smaller dynamic ranges. Since launch in August 1978, the ICE plasma wave instrument never detected stronger signals than those shown here.

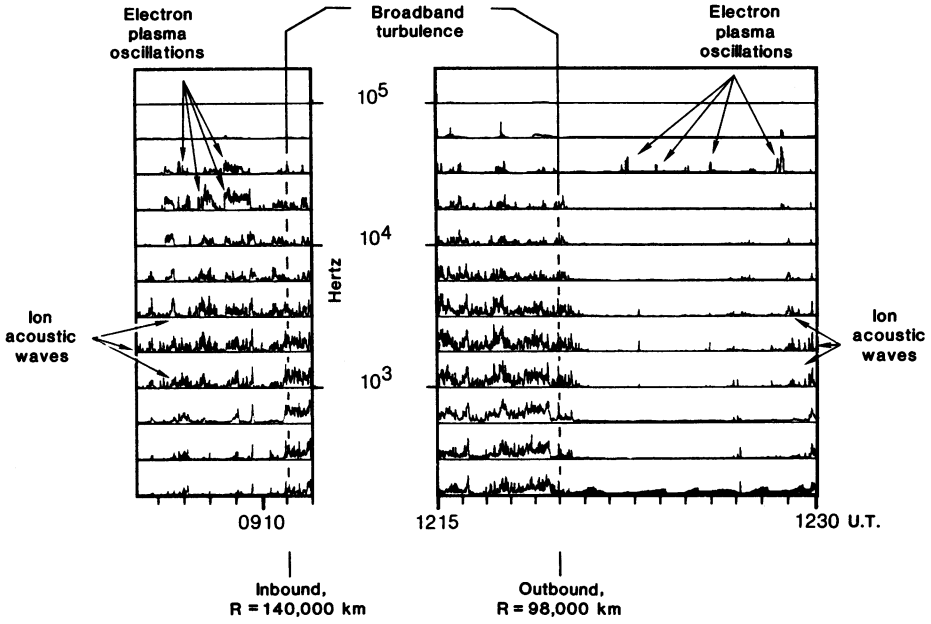

Fig. 3. Detection of thin structures that have characteristics of conventional bow shock traversals (for example, upstream electron plasma oscillations and ion acoustic waves plus broadband turbulence spectra). These shocks or subshocks were detected near the locations predicted by magnetohydrodynamic models, and there were localized changes in electron temperature. However, at least the inbound case did not represent a conventional bow shock encounter.

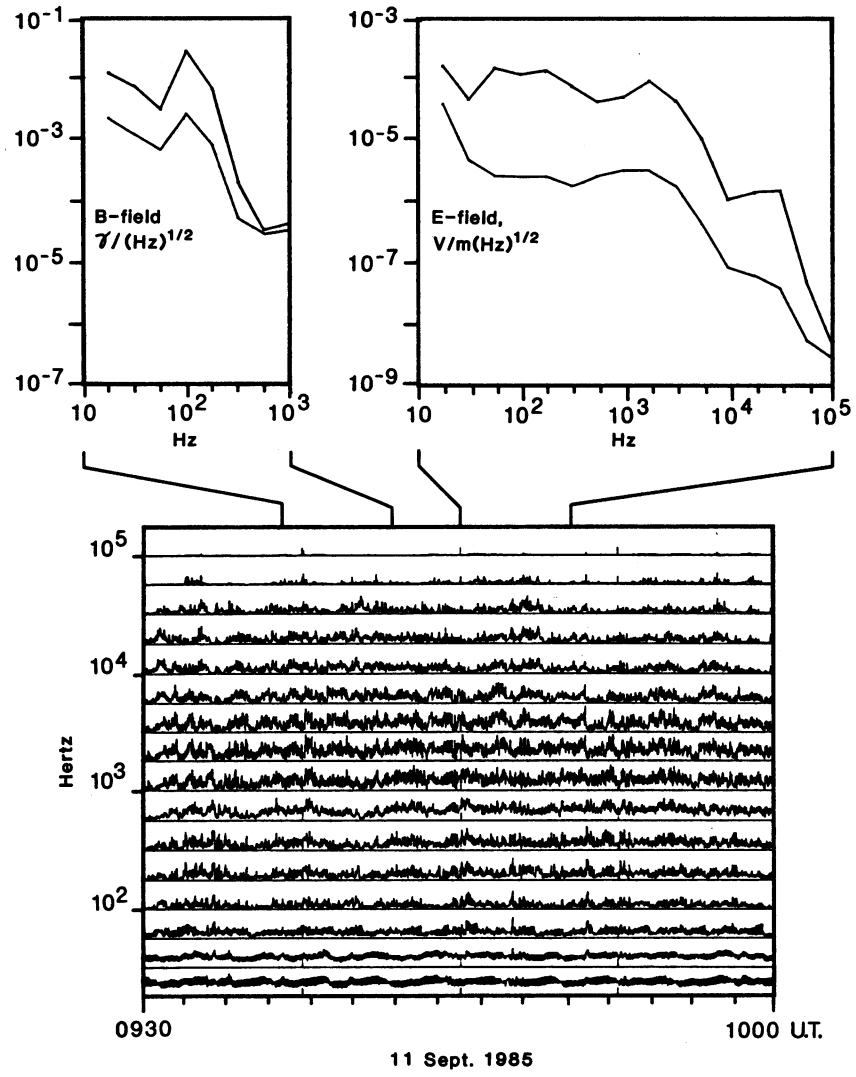

turbulence generated directly by ions from Giacobini-Zinner. The observed size of the turbulent region is consistent with many calculations of the extent of the heavy ion cloud for a comet at 1 astronomical unit (AU).

Strong interaction region. The most intense plasma waves were detected as ICE approached to within a few hundred thousand kilometers of the nucleus. Figure 2 shows the 128-second peak profiles in all 16 E-field channels and in 10 B-field channels for a 10-hour interval centered on closest approach. For each of the E- and B-field channels with frequency $f > 8.8$ Hz, the logarithmic amplitude scale in Fig. 2 (and in Figs. 1, 3, 4, and 5) from the bottom to the top of each channel panel represents an increase of more than nine orders of magnitude in signal intensity. It can be seen that near 0930 to 0945 U.T. and again near 1145 U.T., the 1.8- and 3.1-kHz electric field channels were almost saturated. In fact, the 3.2- and 8.8-Hz magnetic channels did become saturated here; these channels have a more restricted dynamic range, but during the seven previous years of ICE operation within the solar wind and geomagnetic tail, saturation levels were detected rarely. Thus the signals measured by the ICE plasma wave instrument during the comet encounter were as strong as any ever recorded by this instrument.

Before about 0830 U.T. and after 1220 U.T., intense ion acoustic wave ($0.6 < f < 10$ kHz), whistler mode ($f < 100$ Hz) and lower hybrid ($F < 10$ Hz) wave levels were detected as ICE traversed a region with increasing fluxes (*6*) of pickup ions. [Although specific names are used for the plasma wave modes, the wave mode identification is incomplete. The primary basis for identification involves evaluation of the wave frequency in terms of the characteristic frequencies of the plasma (electron and ion cyclotron and plasma frequencies). In addition, we identify electromagnetic modes by examining the search coil response, but have not yet distinguished between modes polarized parallel or perpendicular to the magnetic field.] However, between 0910 and 1020 U.T. and again between 1130 and 1220 U.T., all the wave intensities became much higher. During this time, ICE moved into a region with higher magnetic fields (*8*),

Fig. 4. (Bottom) High-resolution plot of all the individual E-field data points in the region of peak wave turbulence (beyond the visible coma). (Top) Selected E and B spectra showing high peak-to-average ratios and broad frequency extent (for E) and a high whistler mode spectral peak (for B). ICE was evidently in a region of very strong coupling between the comet and the solar wind during this entire period.

increased fluxes of energetic ions (*6*), and increased electron temperatures (*9*). In addition, ions with much higher energies appeared. This may have been associated with the pickup of heavier ions such as CO^+, HCO^+, and the like, since the calculations by Ip (*7*) indicate that the heavy ion population becomes significant at a distance of about 10^5 km. The intense plasma wave activity throughout this inner region suggests that wave-particle interactions contributed significantly to the coupling of solar wind and comet ions, to the heating of the electrons, and to enhancements of the ionization processes, which could produce inhomogeneous flow structures (*10*).

Thin shock-like boundaries were encountered near the boundaries of the regions of maximum plasma wave activity. A cometary bow shock should be affected by heavy ion pickup, which inertially loads (and hence decelerates) the incoming solar wind. The resulting shock is weakened, and it may even disappear if mass loading leads to subsonic flow (*11*). Since a plasma wave instrument detects a characteristic temporal sequence when a planetary bow shock is traversed, the wave observations can provide significant information about the existence and structure of such a collisionless shock at a comet. In fact, from the point of view of the wave measurements alone, we found that normal types of shock structures were detected during the comet encounter. This is illustrated in Fig. 3, in which unaveraged electric field amplitudes are plotted for two short time intervals surrounding the shock crossings. In each case, the upstream region (before 0911 and after 2020 U.T.) has electron plasma oscillations and ion acoustic waves, and the apparent shock crossing is characterized by the presence of broadband impulsive turbulence.

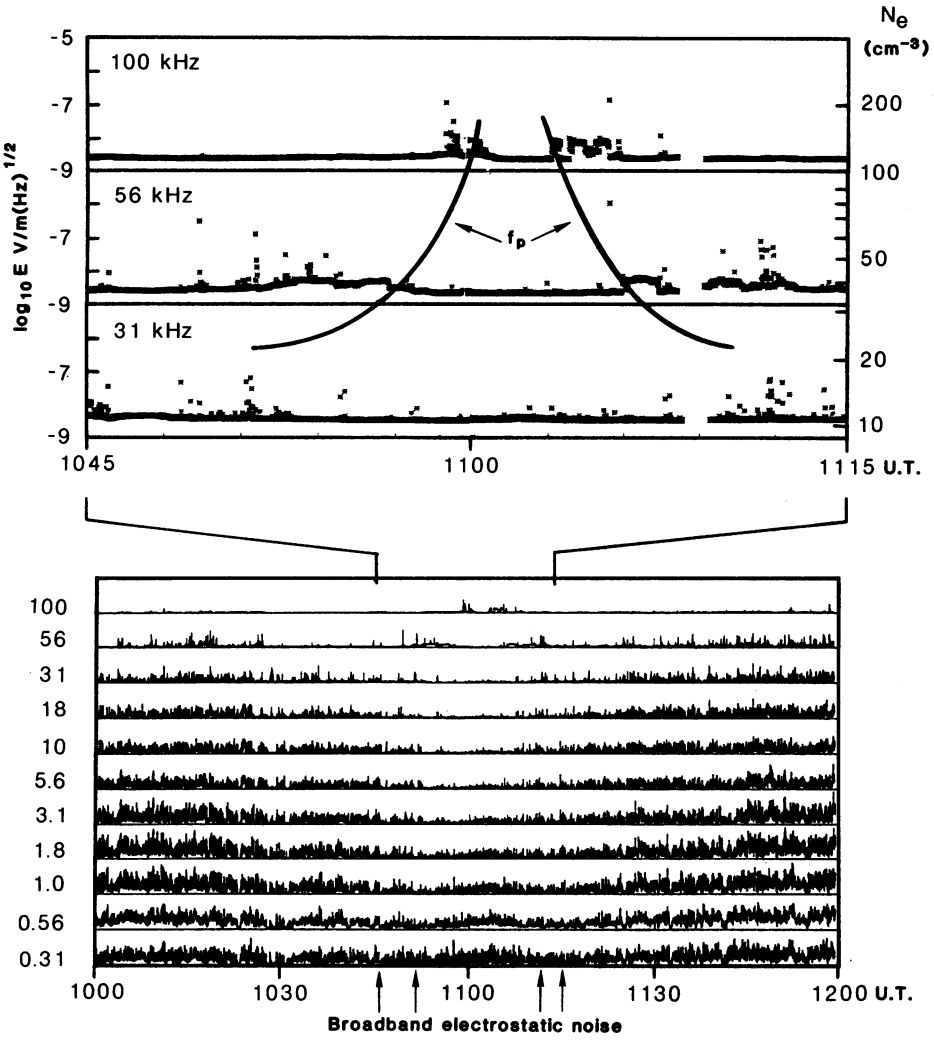

Fig. 5. (Bottom) High-resolution plot showing the general lack of intense mid- and high-frequency electric field turbulence during the crossing of the visible coma (roughly 1032 to 1132 U.T.). The arrows mark regions with broadband electrostatic noise bursts. (Top) Expanded plot of high-frequency measurements showing weak electron plasma oscillations or upper hybrid resonance emissions (see electron density scale on right) that characterize the cold plasma tail of Giacobini-Zinner. Meyer-Vernet *et al.* (*14*) have a comprehensive density plot extending up beyond our range.

For the outbound case there were nearly simultaneous changes in the plasma parameters, magnetic field profile, and energetic ion flux that tend to support the bow shock crossing interpretation. However, for the inbound event there were no rapid changes in magnetic field strength and direction (*8*) or plasma density and velocity (*9*) to support a conventional shock identification; however, there was an increase in electron temperature at 0911 U.T., in coincidence with a broadband noise burst. In fact, for the inbound pass several similar thin wave structures were detected between 0827 and 0911 U.T., but these were related to electron heat conduction variations rather than to temperature changes. Thus for the inbound pass the interaction resembles that found during the AMPTE (active magnetosphere particle tracer explorers) lithium and barium releases, where the detection of intense localized and shock-like plasma wave activity was not well correlated with corresponding changes in other plasma parameters (*12*).

Figure 4 provides more detailed information about the most intense plasma wave activity detected in the region downstream from the inbound shock or subshock. During the interval 0930 to 1000 U.T., the solar wind speed dropped significantly; the solar wind density, temperature, and magnetic field increased in a broad fluctuating transition zone (*8, 9*); and the fluxes of 35- to 240-keV ions increased steadily, peaking at 1005 U.T. (*6*). At this time ICE was in a region of strong coupling between the solar wind and the cometary plasma. These changes are consistent with the concept that, during this particular 30-minute interval, ICE was crossing a thick (38,000 km) and diffuse kind of shock, and the detection of exceedingly high levels of plasma turbulence suggests that significant plasma dissipation occurred in the diffuse shock-like transition.

During this period, the E-field spectrum was very broad, extending from 56 Hz to 56 kHz, and the emissions had an impulsive nature (note the unusually high peak-to-average ratio in the upper spectral plot of Fig. 4). The highest frequency waves (31 and 56 kHz) must be electron plasma oscillations or upper hybrid resonance emissions. Both the peak and average electric field spectra (upper right in Fig. 4) were remarkably flat from 56 Hz to 1.8 kHz; the secondary spectral peak at 31 kHz was near the local electron plasma frequency for the selected 5-minute interval. In the wave magnetic field spectrum in Fig. 4, the 100-Hz peak corresponds to about 0.2 to 0.25 of the local electron cyclotron frequency, which suggests that the waves were in the whistler mode. Whistlers are typically generated by a

distribution of superthermal electrons with higher fluxes perpendicular to the magnetic field than parallel to the field (*13*). For $B = 18$ nT and $N = 10$ cm^{-3}, such electrons would need parallel energies near (f_c/f) $(B^2/8\pi N) = 140$ eV to excite the observed whistlers (B is magnetic field strength, f_c is electron cyclotron frequency, N is electron density, and f is the measured wave frequency). This value for the parallel energy is higher than the measured thermal energy by a factor of about 4 (*9*). The quasi-linear pitch angle scattering time would be about 300 seconds based on use of the average wave amplitude.

The electric oscillations with $f < 10$ kHz may have been generated by cross-field beam or anisotropy instabilities associated with cometary ions. These waves also interact with electrons, and a quasi-linear estimate gives an electron scattering or heating time of approximately 1500 seconds. If electrons could be contained in the interaction region for a comparable time, then this mid-frequency electric field turbulence could significantly affect the electron energy balance.

Coma and tail. The visible coma of comet Giacobini-Zinner was traversed in a period of slightly less than 1 hour centered around 1102 U.T. The inner coma contained relatively low levels of plasma wave activity (Fig. 5). However as ICE traversed this quiet plasma region, the two wave instruments detected signals that provided unique information about the characteristics of the cold plasma tail.

The lower panel in Fig. 5 shows distinct high-frequency activity between about 1045 and 1115 U.T., and the upper panel contains an expanded plot of the E-field amplitudes in the top three plasma wave channels. We assume that these emissions are at the electron plasma frequency, and the scale on the right then gives equivalent electron density. The simplified profile for the electron plasma frequency, f_p, can be used to derive $N(t)$ or $N(z)$, where z is the distance across the tail; thus, we find that the 30 cm^{-3} density level of the tail was traversed in about 11.5 minutes, corresponding to a distance of 15,000 km, while the central "core" with $N > 120$ cm^{-3} had a thickness of only about 4000 km. The 24-channel ICE radio mapping investigation has overlapping coverage down to 30 kHz and many additional channels extending up to 2 MHz. Meyer-Vernet *et al.* (*14*) used their high-sensitivity and high-frequency resolution to derive a detailed profile of the plasma temperature and density throughout the tail crossing. Although the radio profile shows more structure than the one plotted here, the two sets of measurements appear to be in agreement. For instance, the 100-kHz response between 1103 and 1106 U.T. shows several peaks, and the structured density profile of Meyer-Vernet *et al.* shows several excursions through the $N = 123$ cm^{-3} level here.

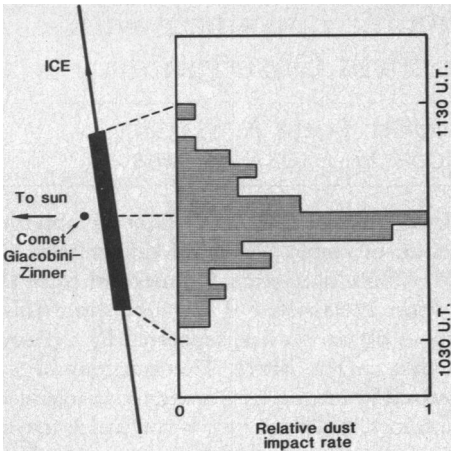

Fig. 6. ICE trajectory, as seen by a ground-based viewer, together with a plot of the relative rate of dust impacts detected by the plasma wave instrument.

In Earth's magnetosphere and in the plasma environment of Venus, the tail boundary is generally characterized by the presence of broadband electrostatic noise (*15*), and similar waves were detected at Titan (*3*). The bottom panel in Fig. 5 shows several broadband noise bursts that could represent the comet tail boundary in a similar way. If this interpretation is correct, then it suggests that the comet tail had a width of more than 32,000 km along the ICE trajectory.

Cometary dust. During the 1-hour crossing of the coma region, the ICE plasma wave instrument also detected relatively few isolated impulses. These signals had spectral characteristics similar to plasma wave impulses detected when Voyager 2 crossed Saturn's ring plane. These were subsequently interpreted as dust impacts from the G ring (*4*); similarly, we interpret the ICE impulses in terms of the crossing of the Giacobini-Zinner dust tail. Figure 6 shows the spacecraft trajectory as seen from Earth, along with a preliminary normalized profile of dust impacts across the comet tail; the term "preliminary" is used here because quantitative tests to distinguish between dust impacts and plasma wave bursts have not been applied, and we have not inserted dead-time correction. However, it can already be stated that the peak impact rate was low (on the order of one hit every few seconds). In fact, the profile in Fig. 6 is in rough agreement with the "smallest dust envelope" reported earlier (*16*), and the lack of degradation in the ICE solar array output is consistent with the low impact rate measured by the plasma wave instrument.

Conclusion. The comet literature contains many theoretical suggestions involving the generation of various plasma instabilities by the interaction of newly ionized cometary gases with the solar wind (*10*). These proposed instabilities have different functions; some address issues of ion momentum coupling and some are related to phenomena involving ionization and electron heating. The preliminary analysis presented here illustrates the impressive degree to which plasma physics phenomena associated with such instabilities and wave-particle interactions mediate the comet–solar wind interaction over a region that extends far beyond the visible comet boundary.

REFERENCES AND NOTES

1. F. L. Scarf, E. J. Smith, R. Farquhar, in *Cometary Exploration*, T. I. Gombosi, Ed. (Hungarian Academy of Sciences, Budapest, 1983), vol. 2, p. 225.
2. F. L. Scarf, D. A. Gurnett, W. S. Kurth, *Science* **204**, 991 (1979); J. W. Warwick *et al.*, *ibid.* p. 995.
3. D. A. Gurnett, W. S. Kurth, F. L. Scarf, *ibid.* **212**, 235 (1981); J. W. Warwick *et al.*, *ibid.*, p. 239.
4. F. L. Scarf, D. A. Gurnett, W. S. Kurth, R. L. Poynter, *ibid.* **215**, 587 (1982); D. A. Gurnett, E. Grun, D. Gallagher, W. S. Kurth, F. L. Scarf, *Icarus* **53**, 236 (1983).
5. A complete description of the ICE plasma wave instrument may be found in F. L. Scarf, R. W. Fredricks, D. A. Gurnett, B. J. Smith, *IEEE Trans. Geosci. Electron.* GE-16, 225 (1978).
6. R. J. Hynds *et al.*, *Science* **232**, 361 (1986); F. M. Ipavich *et al.*, *ibid.*, p. 366.
7. W.-H. Ip, *Astron. Astrophys.* **92**, 95 (1980); D. A. Mendis and H. L. F. Houpis, *Rev. Geophys. Space Phys.* **20**, 885 (1982).
8. E. J. Smith *et al.*, *Science* **232**, 382 (1986).
9. S. J. Bame *et al.*, *ibid.*, p. 356.
10. C. S. Wu and R. C. Davidson, *J. Geophys. Res.* **77**, 5399 (1972); R. E. Hartle and C. S. Wu, *ibid.* **78**, 5802 (1973); D. Winske, C. S. Wu, Y. Y. Li, Z. Z. Mou, S. Y. Guo, *ibid.* **90**, 2713 (1985); V. Formisano, A. A. Galeev, R. Z. Sagdeev, *Planet Space Sci.* **30**, 491 (1982); K. Papadopoulos, *Radio Sci.* **19**, 571 (1984).
11. H. U. Schmidt and R. Wegmann, in *Comets*, L. L. Wilkening, Ed. (Univ. of Arizona Press, Tucson, 1982), p. 538; A. A. Galeev, T. E. Cravens, T. I. Gombosi, *Astrophys. J.* **289**, 807 (1985).
12. D. A. Gurnett *et al.*, *J. Geophys. Res.* **91**, 1301 (1986); D. A. Gurnett *et al.*, *Geophys. Res. Lett.* **12**, 851 (1985).
13. C. F. Kennel and H. E. Petschek, *J. Geophys. Res.* **71**, 1 (1966).
14. N. Meyer-Vernet *et al.*, *Science* **232**, 370 (1986).
15. D. A. Gurnett, L. A. Frank, R. P. Lepping, *J. Geophys. Res.* **81**, 6059 (1976); F. L. Scarf *et al.*, *Geophys. Res. Lett.* **11**, 335 (1984); D. S. Intriligator and F. L. Scarf, *J. Geophys. Res.* **89**, 47 (1984).
16. D. K. Yeomans and J. C. Brandt, *The Comet Giacobini-Zinner Handbook* (Jet Propulsion Laboratory, Pasadena, CA, 1985).

17. The plasma wave team found it a great experience to participate in the first comet encounter mission and want to express their deepest gratitude to many key individuals from the ICE Project Team, many others on the staff of Goddard Space Flight Center and its National Space Science Data Center, NASA's Deep Space Network, the ICE supporters at NASA Headquarters, and those International Halley Watch participants who kept us so well informed as the spacecraft and comet closed in on each other. We thank A. Fujinami for his assistance and we express our special gratitude to S. Chang for her outstanding and dedicated technical support during the many months leading up to 11 September, and during the week of encounter. The research at TRW was supported by NASA under contract NAS5-28703 and the research at the University of Iowa was supported under contract NAS5-28701.

20 September 1985; accepted 29 January 1986

Plasma Wave Observations at Comet Giacobini-Zinner

FREDERICK L. SCARF, FERDINAND V. CORONITI, CHARLES F. KENNEL, DONALD A. GURNETT, WING-HUEN IP and EDWARD J. SMITH

Science **232** (4748), 377-381.
DOI: 10.1126/science.232.4748.377